Letters in Applied NanoBioScience
Open-Access Journal (ISSN: 2284-6808)

Article
Volume 14, Issue 1, 2025, 31
https://doi.org/10.33263/LIANBS141.031

In Silico Screening of Biological Activity of S-R-4-N-Halogenacylaminobenzenesulfonothioates

Nazarii Kopak [1], Sofia Vasyliuk [1,*]

[1] Department of Technology of Biologically Active Compounds, Pharmacy and Biotechnology, Lviv National Polytechnic University, S. Bandery Str. 12, Lviv, Ukraine; nazarii.a.kopak@lpnu.ua (N.K.), sofiia.v.vasyliuk@lpnu.ua (S.V.);
* Correspondence: sofiia.v.vasyliuk@lpnu.ua (S.V.);

Scopus Author ID 12768497000

Received: 22.12.2023; Accepted: 1.03.2024; Published: 27.09.2024

Abstract: This research focuses on S-R-4-N- halogenacylaminobenzenesulfonothioates, obtained from the Department of Technologies of Biologically Active Compounds, their predicted biological activity using virtual screening tools, including SuperPred web server and molecular docking. Molecular docking studies were conducted with AutoDock Vina software to identify substances with potential efficacy against COVID-19 and swine influenza (H1N1). Additional calculations were made according to Lipinski's rules (lipophilicity, hydrogen bond acceptors, molecular weight, and number of rotational bonds). The 3D structures of compounds and targets were presented using the Biovia program. Our research explored the bioactivity of specific compounds, focusing on their antiviral and antimicrobial potential and broad biological activity. Among these compounds, S-Methyl-4-[(trifluoroacetyl)amino]-benzenesulfonothioate (1a) and S-(4-Nitrophenyl)-4-[(3-chloropropanoyl) amino]-benzenesulfonothioate (2g) demonstrated high affinity with the 6LU7 (COVID-19) and 3AL4 (H1N1) proteins and emerged as a lead candidate for experimental research in the development of an effective COVID-19 treatment. Using the SuperPred web server, we predicted its potential to bind with COVID-19 and H1N1-related targets. This study offers potential as a non-toxic drug with antimicrobial and antiviral properties, as indicated by our virtual screening and molecular docking studies. The identification of lead compounds (1a, 2g) offers a compelling starting point for experimental research, potentially advancing drug discovery and repurposing efforts for therapeutic applications.

Keywords: S-esters thiosulfoacids; molecular docking; virtual screening; biological activity; Lipinski's rule.

1. Introduction

In a continuously changing modern world, the human population is confronted with a diverse range of significant concerns that require urgent consideration. One notable difficulty that is now being faced is the increasing incidence of viral illnesses, which has led to a need for the exploration of novel and secure antiviral medicines. The progress made in treating viral infections has faced major challenges, principally due to the complex characteristics of viral nature, which differ considerably from those of bacterial illnesses. Currently, antiviral drugs frequently demonstrate insufficient efficacy in achieving total eradication of viruses, instead providing limited alleviation through symptom mitigation and reduction of fatality rates. The intricacy of this undertaking is further compounded by the increased vulnerability to bacterial and fungal infections caused by impaired immunity as a consequence of viral infections. It is worth mentioning that the occurrence of secondary infections, such as mucormycosis and

aspergillosis, in patients with COVID-19 has introduced further intricacies in managing the condition [1].

Therefore, there is a pressing necessity to identify innovative, non-toxic pharmaceuticals that possess potent antiviral and antibacterial characteristics.

Current research endeavors have primarily concentrated on organosulfur compounds, particularly those that possess -S-S-disulfide bonds. These molecules have exhibited diverse applicability across multiple domains [2,3].

This article explores the biological properties of S-esters thiosulfoacids. Significant efforts have been made to create synthetic methods for thiosulfonates due to their extensive use. Most often, they are obtained by oxidation of disulfides, sulfenylation of salts of sulfinic acids with alkyl halides, sodium or potassium salts of thiosulfonic acids with alkyl halides, oxidation of thiols, decomposition of sulfonyl hydrazides, reduction of sulfonyl chlorides [2–4].

The selection of these compounds has been based on their possible antibacterial capabilities; nevertheless, their potential applications extend beyond this particular element. Numerous studies have confirmed that several synthetic thiosulfoesters manifest a wide range of biological activities, such as their ability to inhibit blood clot formation [5], capacity to neutralize harmful free radicals [6], efficacy against parasites [7], and potential as anti-cancer agents [8].

In addition, thiosulfoesters show a wide spectrum of antibacterial and antifungal activity [6, 9–11]. Therefore, they are promising for searching for drugs with simultaneous antiviral and antifungal or antibacterial effects.

2. Materials and Methods

The physicochemical and certain antibacterial properties of S-R-4-N-halogenacylaminobenzenesulfonothioates received at the Department of Technologies of Biologically Active Compounds of Pharmacy and Production Biotechnology are detailed in the work [10].

Prediction of the biological activity of S-R-4-N-halogenacylaminobenzenesulfonothioates was investigated using the SuperPred web server [12–14].

The parameters of compounds (lipophilicity, hydrogen bond acceptors, molecular weight, and number of rotational bonds) were calculated using the Molinspiration program [15, 16] in accordance with Lipinski's criteria [17].

The Biovia software was utilized to display the three-dimensional configuration of compounds and targets and simulate chemical bond formation during the molecular docking procedure [18].

The molecular docking process utilized the AutoDock Vina program [19].

The AutoDock Vina (version 1.1.2) software was used to determine the molecular interaction of ligands with target proteins based on scoring function and rapid gradient optimization conformational search. Proteins in PDB file format were uploaded to the BIOVIA Discovery Studio, where ligands, targets, and binding sites were defined. After that, prepared molecules were uploaded to AutoDock Vina software, and sphere dimensions were chosen for docking at the binding site.

X, Y, and Z coordinates were obtained from binding sphere properties from BIOVIA studio and written in the config file for AutoDock Vina software. The binding energy,

conventional hydrogen bond, and other interactions were calculated and visualized by BIOVIA Discovery Studio 2021 software [20]. AutoDock Vina calculates the docking scoring function by the following formula:

$$\Delta G_{binding} = {}_{c1}\Delta G_{ydw} + {}_{c2}\Delta G_{Hbond} + {}_{c3}\Delta G_{entropy}, \quad (1)$$

where the c1, c2, and c3 are the coefficients obtained from the respective ΔG term [21].

3. Results and Discussion

Among S-R-4-N-halogenacylaminobenzenesulfonothioates, compounds 1a, 1b, and 2a-2g were selected as objects of research in our work (Figure 1).

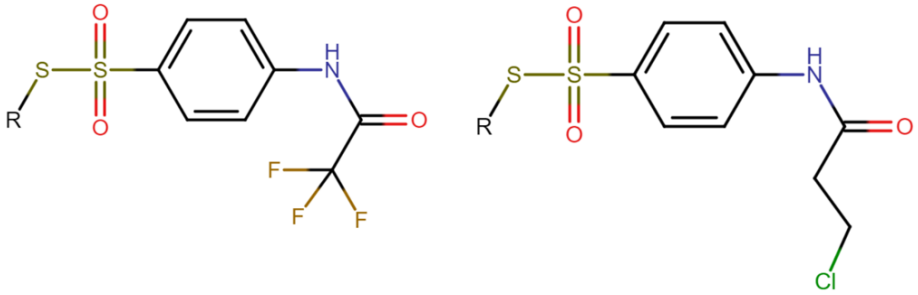

(1) **(2)**

Figure 1. S-R-4-N- halogenacylaminobenzenesulfonothioates

1a CH_3
1b C_2H_5

2a CH_3
2b C_3H_7
2c i-C_3H_7
2d C_4H_9
2e C_6H_5
2f C_6H_4Cl-4
2g $C_6H_4NO_2$-4

Initial studies of their antibacterial and antifungal activities have shown that they are promising targets for their potential antiviral activity. The search for potential antiviral drugs with simultaneous antibacterial and antifungal effects among these compounds can be justified by the rather simple procedure of their preparation and the presence of primary biological research confirming their antibacterial activity [10].

Thiosulfoesters **1a** and **1b** can be synthesized by acylating alkyl esters of 4-aminobenzenethiosulfoacid **1a** and **1b** with trifluoroacetic anhydride in benzene. The reaction was carried out at an equimolar ratio of reactants and the boiling temperature of the reaction mixture, resulting in a virtually quantitative yield of 90-95% [10].

The S-esters of 4-(3-chloropropionylamino)-benzenethiosulfoacid **2a-2g** can be synthesized with somewhat lower yields. This was achieved by acylating the corresponding esters of 4-aminobenzenethiosulfoacid using the chloroanhydride of *β*-chloropropionic acid in dioxane, with the presence of pyridine [10].

Regarding their antibacterial and antifungal activity, these compounds were found to be active against the following bacteria and fungi: *Candida tenuis*, *Aspergillus niger*, *Penicillium chrysogenum*, *Escherichia coli*, *Bacillus mesentericus*, *Staphylococcus aureus*, *Mycobacterium luteum*, *Candida albicans*, *Candida glabrata*, *Aspergillus fumigatus*, *Verticillium dahliae*, *Trichophyton gypseum*; *E: Pseudomonas aeruginosa*; *F: Bacillus subtilis*; *I: Proteus vulgaris* [10].

Since experimental biological research is a very time-consuming and expensive process, virtual screening is an effective method of finding the most promising compounds, reducing the time and cost of research. Also, the quantity of experimental animals needed for biological study is reduced, as chemicals with minimal action are eliminated during the screening phase. Computer programs for screening make it possible to increase the effectiveness of the research of the obtained compounds, so we decided to study them using the in silico method.

Before making predictions about the activities of the chosen research objects in applications for molecular docking and visualization, it is important to check whether the provided compounds satisfy the criteria stated in the Lipinski rules (Table 1). The computations were performed with the Molinspiration Cheminformatics Software [15].

Table 1. Compounds properties calculations results.

Compound	Log P	Molecular polar surface, Å^2	Molecular weight	The number of non-hydrogen atoms	Molecular volume, Å^3	Number of hydrogen bond acceptors (O and N atoms)	Number of hydrogen bond donors (NH and OH groups)	The number of rotating connections
1a	1,85	63,24	299,30	18	212,85	4	1	4
1b	2.23	63.24	313.32	19	229.65	4	1	5
2a	1.80	63.24	293.80	17	228.69	4	1	5
2d	2.68	63.24	321.85	19	262.29	4	1	7
2e	2.54	63.24	321.85	19	262.08	4	1	6
2f	3.24	63.24	335.88	20	279.10	4	1	8
2l	3.33	63.24	355.87	22	283.54	4	1	6
2m	4.01	63.24	390.31	23	297.07	4	1	6
2n	3.29	109.06	400.87	25	306.87	7	1	7

The calculation of LogP is determined using the process established by Molinspiration, which involves summing fragment-based contributions and applying correction factors. The method is highly resilient and capable of processing nearly all organic compounds, as well as the majority of organometallic substances. The molecular polar surface area is determined by adding together the contributions of individual fragments. N- and O-centered polar pieces are taken into account. The polar surface area has demonstrated excellent efficacy in describing drug absorption, encompassing intestinal absorption, bioavailability, and blood-brain barrier penetration [16]. The molecular volume is determined by calculating the sum of the contributions of each fragment to the actual three-dimensional volume of a training set consisting of approximately twelve thousand molecules. The number of rotatable bonds is a basic topological quantity that quantifies the flexibility of a molecule. It demonstrated that it is an excellent indicator of how much medications can be absorbed and utilized in the body through oral administration [22].

Requirements for the compounds by Lipinski [17]:

- No more than 5 hydrogen bond donors
- No more than 10 hydrogen bond acceptors (all nitrogen or oxygen atoms)
- Molecular mass is less than 500 daltons
- Calculated lipophilicity (log *P*) is less than 5
- No more than 10 rotational bonds

Following the analysis of the data presented in the table, it is evident that all the compounds under study adhere to Lipinski's rules, commonly referred to as the Rule of Five in

drug discovery. Lipinski's rules, introduced by Christopher A. Lipinski in 1997, provide a framework for evaluating the drug-likeness of compounds based on their physicochemical properties. These rules emphasize specific criteria related to molecular weight, lipophilicity, hydrogen bond donors, and acceptors [17]. For our studied compounds, we obtained molecular weight in 293.80 – 400.87, lipophilicity in 1.80 – 4.01, and hydrogen bond acceptors 4 – 7. All compounds have 1 hydrogen donor. By meeting these criteria, compounds are more likely to possess characteristics conducive to oral bioavailability and efficacy, which are crucial in the early stages of drug discovery. Adherence to Lipinski's rules significantly indicates a compound's potential as a drug candidate, simplifying the initial screening process and enhancing the probability of successful drug development.

The utilization of SuperPred's web server predictions can greatly assist researchers and scientists in comprehending the metabolic pathways of certain compounds within the human body. This knowledge has significant importance in the realms of medication development, toxicology investigations, and the evaluation of potential dangers linked to chemical exposure. The dataset for the target prediction was obtained from the ChEMBL database. The prediction method of the SuperPred web server has been completely reworked and is now based on machine learning models instead of overall structural similarity. This allows for the accurate prediction of ATC groups, even in cases where only small parts of the respective structures, such as functional groups, are responsible for the therapeutic impact or metabolic processes and, therefore, the assignment to a specific ATC code. By these means, the accuracy of the ATC prediction could be improved by more than five percent compared to the previous version of the web server [13].

Prediction of (therapeutic) targets is no longer based only on active binders but also includes experimentally confirmed nonbinders extracted from the ChEMBL database. Together with the machine learning methodology, this design enables a much more accurate assessment of structural groups that play a role in the protein binding process, in addition to the advantage that focusing on substructure features in contrast to overall structural similarity already offers. Furthermore, the previous scoring function was replaced with more intuitive values, which are easily assessable at first glance [13].

Possible relevant indications for predicted targets were extracted from the Therapeutics Target Database (TTD, [23]). Each of the included predictable targets was mapped to targets in the TTD database, and their associated indications are displayed in a separate table if the respective target is predicted to be active for a structure of interest. Suppose multiple indications are assigned to a single target. In that case, each indication is displayed in a separate row to facilitate searching the table for indications that are shared between multiple different predicted targets.

As shown in Table 2 the screening results indicate that among the examined library of S-R-4-N- halogenacylaminobenzenesulfonothioates, the compounds with the highest potential for the discovery of antiviral medicines targeting the COVID-19 virus are as follows: the compounds **2f**, **2c**, and **2g** are identified as S-(4-Chlorophenyl) 4-[(3-chloro propanoyl)amino]benzenesulfonothioate, S-(1-Methylethyl) 4-[(3-chloro propanoyl)amino]benzenesulfonothioate, and S-(4-Nitrophenyl) 4-[(3-chloro propanoyl)amino]benzenesulfonothioate, respectively. These compounds exhibit potential activities of 63.92%, 62.66%, and 60.93%, respectively.

Table 2. Prediction of biological activities using SuperPred web server.

Compound	Target name	Indication	Probability (%)	Model accuracy (%)
1a	Sodium channel protein type III alpha subunit	Angina pectoris [ICD-11: BA40]	90.71	96.9
	Cyclin-dependent kinase 1/cyclin B1	Acute lymphoblastic leukaemia [ICD-11: 2A85]	86.49	91.24
	Adenosine A2b receptor	Herpes simplex virus infection [ICD-11: 1F00]	63.47	98.59
	Serine/threonine-protein kinase mTOR	Coronavirus Disease 2019 (COVID-19) [ICD-11: 1D6Y]	54.41	92.78
1b	Sodium channel protein type III alpha subunit	Angina pectoris [ICD-11: BA40]	90.66	96.9
	PI3-kinase p110-alpha/p85-alpha	Breast cancer [ICD-11: 2C60-2C65]	89.64	94.33
	Cyclin-dependent kinase 1/cyclin B1	Breast cancer [ICD-11: 2C60-2C65]	89.01	91.24
	Epoxide hydratase	Chronic obstructive pulmonary disease [ICD-11: CA22]	87.14	94.09
2a	PI3-kinase p110-alpha/p85-alpha	Breast cancer [ICD-11: 2C60-2C65]	87.68	94.33
	Adenosine A2b receptor	Herpes simplex virus infection [ICD-11: 1F00]	81.28	98.59
	CDK2/Cyclin A	Thymic cancer [ICD-11: 2C27]	80.51	91.38
	Serine/threonine-protein kinase mTOR	Coronavirus Disease 2019 (COVID-19) [ICD-11: 1D6Y]	56.31	92.78
2d	Cyclin-dependent kinase 1/cyclin B1	Solid tumor/cancer [ICD-11: 2A00-2F9Z]	90.13	91.24
	Adenosine A2b receptor	Herpes simplex virus infection [ICD-11: 1F00]	90.06	98.59
	Cystic fibrosis transmembrane conductance regulator	HIV-associated diarrhoea [ICD-11: 1A2Z]	58.76	95.71
	Adenosine A3 receptor	Hepatitis C virus infection [ICD-11: 1E51.1]	51.63	95.93
2e	Adenosine A2b receptor	Herpes simplex virus infection [ICD-11: 1F00]	85.67	98.59
	C-X-C chemokine receptor type 4	Human immunodeficiency virus infection [ICD-11: 1C62]	75.08	93.1
	Serine/threonine-protein kinase mTOR	Coronavirus Disease 2019 (COVID-19) [ICD-11: 1D6Y]	62.66	92.78
2f	Adenosine A2b receptor	Herpes simplex virus infection [ICD-11: 1F00]	89.1	98.59
	Cystic fibrosis transmembrane conductance regulator	HIV-associated diarrhoea [ICD-11: 1A2Z]	62.38	95.71
	DNA topoisomerase I	Human immunodeficiency virus infection [ICD-11: 1C62]	61.53	97
	Serine/threonine-protein kinase mTOR	Coronavirus Disease 2019 (COVID-19) [ICD-11: 1D6Y]	52.64	92.78
2l	Glutathione S-transferase Pi	Solid tumor/cancer [ICD-11: 2A00-2F9Z]	86.41	93.81
	PI3-kinase p110-alpha/p85-alpha	Solid tumor/cancer [ICD-11: 2A00-2F9Z]	71.38	94.33
	Muscarinic acetylcholine receptor M5	Allergic rhinitis [ICD-11: CA08.0]	69.8	94.62
2m	Adenosine A2b receptor	Herpes simplex virus infection [ICD-11: 1F00]	85.76	98.59
	Cyclin-dependent kinase 1/cyclin B1	Solid tumor/cancer [ICD-11: 2A00-2F9Z]	82.73	91.24
	Bromodomain-containing protein 2	Coronavirus Disease 2019 (COVID-19) [ICD-11: 1D6Y]	63.92	86.19
2n	PI3-kinase p110-alpha/p85-alpha	Breast cancer [ICD-11: 2C60-2C65]	89	94.33
	Adenosine A2b receptor	Herpes simplex virus infection [ICD-11: 1F00]	84.11	98.59
	Serine/threonine-protein kinase mTOR	Coronavirus Disease 2019 (COVID-19) [ICD-11: 1D6Y]	60.93	92.78

Furthermore, it was discovered that **2b** - S-Propyl 4-[(3-chloropropanoyl) amino] benzenesulfonothioate and **2d** S-Butyl 4-[(3-chloropropanoyl) amino] benzenesulfonothioate exhibited antiviral activity against herpes simplex virus with a probability of 90.06% and 89.1%, respectively.

It is noteworthy that during the screening phase, several compounds with potential anticancer characteristics were identified. Compounds, namely **1b** - S-Ethyl 4-[(trifluoroacetyl) amino] benzenesulfonothioate and **2a** - S-Methyl 4-[(3-chloropropanoyl) amino] benzenesulfonothioate, exhibited promising efficacy against breast cancer, with probabilities of 89.64% and 81.28% respectively.

Among the various methods utilized in computational chemistry, molecular docking stands out as one of the most informative and reliable. It estimates how a ligand, or a drug molecule, interacts with its target, the receptor. Accurate predictions of these interactions are crucial for the development of effective drugs.

However, it is important to note that molecular docking does not account for other crucial phases of a drug's lifecycle within the body. It doesn't consider aspects such as the drug's absorption into the bloodstream, its metabolism or transformation within the body, its subsequent excretion, or its potential toxicity.

While the aforementioned processes are all critical parts of a drug's journey, the ligand's binding with the receptor triggers the physiological reaction – the ultimate purpose of administering the drug. Molecular docking contributes significantly to our understanding of how and why a drug works by accurately predicting this binding.

The selection of swine influenza (H1N1) and COVID-19 as subjects for docking studies is motivated by their significant impact on global health, aiming to elucidate potential therapeutic interventions through molecular docking. This choice is underscored by the pressing need to comprehend the molecular interactions of these viruses with compounds, paving the way for targeted drug design and discovery. Both swine influenza (H1N1) and COVID-19 are zoonotic diseases capable of spreading rapidly among humans and causing global pandemics. These viruses exhibit high rates of transmission, making them a significant public health concern, potentially leading to widespread infections and severe health complications. Swine influenza (H1N1) and COVID-19 can lead to severe respiratory illness, hospitalizations, and, in some cases, fatalities.

As with all the enveloped viruses, the entry of influenza includes several steps in host cell infection. Hemagglutinin (HA) protein plays an important role in this process. HA is a trimeric glycoprotein present in multiple copies in the membrane envelope of the influenza virus. HA contains a fusion peptide, a receptor binding site, a metastable structural motif, and the transmembrane domain. The first step of influenza virus entry is the recognition of the host cell receptor molecule, terminal α-sialic acid, by HA. This multivalent attachment by multiple copies of trimetric HA triggers the endocytosis of the influenza virus contained in the endosome. The endosome-trapped virus traffics via a unidirectional pathway near the nucleus. At this location, the endosome's interior pH becomes acidic, which induces a dramatic conformational change in HA to insert the fusion peptide into the host membrane, juxtapose the two membranes, and form a fusion pore that allows the release of the genome segments of the influenza virus. HA plays a key role in the entire entry pathway. Inhibitors of virus entry are potentially effective antiviral drugs for influenza viruses [24].

The active site of the 6LU7 structure has a covalent inhibitor (N3) that forms critical interactions with the protease. The N3 inhibitor establishes a covalent interaction with the sulfur atom located at position Cys145. In addition, it establishes considerable hydrogen bonds with Gly143, Ser144, and Cys145, as well as with the catalytic residue His41. This serves as a noteworthy illustration of the potential crucial interactions that can be utilized in developing protease inhibitors [25].

In the molecular docking study, leveraging a scoring function and rapid gradient optimization conformational search, ligand-protein interactions were examined with proteins 6LU7 [26] and 3AL4 [27]. Subsequently, prepared ligand molecules were subjected to docking simulations using AutoDock Vina software. The chosen docking parameters included a cubic binding site with dimensions of 30 × 30 × 30 Å. For the 3AL4 protein, the binding site was centered at coordinates (center_x = -74.693952, center_y = -79.661667, center_z = -11.728837), while for the 6LU7 protein, it was centered at coordinates (center_x = -10.729204, center_y = 12.417653, center_z = 68.816122). The protein target preparation process involved the addition of polar hydrogen atoms, removing water molecules, and incorporating Kollman charges to optimize the protein structures for accurate molecular docking assessments, as detailed in the methodology [28]. Polar hydrogen atoms typically participate in hydrogen bonding, resulting in dipole-dipole and other weak intermolecular interactions. In contrast, non-polar hydrogens engage in van der Waals interactions with relatively limited impact. The significance of this phenomenon lies in its relevance to biological interactions, namely those involving a medication and its target receptor. In such interactions, the electrostatic potential plays a crucial role in determining the probability and intensity of the contact [29]. The BIOVIA Discovery Studio program [18] was utilized to create the active binding zones of the protein receptor and visualize the final results.

Docking analyses were conducted on the primary protease of COVID-19 in conjunction with the inhibitor N3 [26] and swine-origin A (H1N1)-2009 influenza A virus hemagglutinin (HA) with NAG ligand (2-acetamido-2-deoxy-beta-D-glucopyranose) [27]. The 6LU7 represents a distinct conformation of the major protease (Mpro) of the SARS-CoV-2 virus, which holds significant importance in the virus's life cycle. Therefore, it has emerged as a primary objective for prospective therapeutic development endeavors to combat COVID-19. The protease plays a crucial role in the enzymatic cleavage of the polyproteins synthesized from the viral RNA. Hemagglutinin (HA) has been associated with the airborne transmission of influenza A viruses [30].

Table 3. The results of the Gscore summary function of the conducted docking studies of given compounds against swine influenza (H1N1) target 3AL4.

Compound	ligand	1a	1b	2a	2b	2c	2d	2e	2f	2g
Affinity (kcal/mol)	-5.1	-5.2	-5.3	-4.9	-5.1	-5.1	-5.1	-5.3	-5.4	-5.6

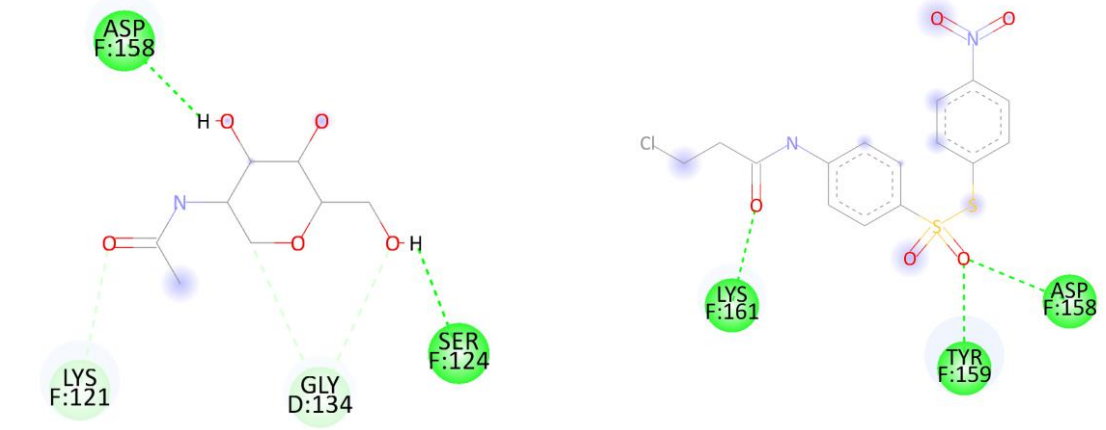

(a) **(b)**

Figure 2. (a) 2D interactions of native ligand with target protein 3AL4; (**b**) 2D interactions of **2g** with target protein 3AL4.

The results of screening the biological activity of thiosulfoesters **1a-1b** and **2a-2g** using molecular docking indicate the high feasibility of searching for new antivirus drugs against swine influenza (H1N1) targets among the investigated thiosulfoesters. The most promising in this plan of research may be the hit compound "**2g**" - S-(4-Nitrophenyl) 4 - [(3-chloropropanoyl)amino] benzenesulfonothioate. Affinity value was calculated at a level of -5.6 kcal/mol, which was higher than that of the native ligand, which was -5.1 kcal/mol (Table 3). The sulfo group established a bond with ASP F:158 and TYR F:159 via conventional hydrogen bonds. LYS F:161 is also holding 3 chlorine propionyl fragments via conventional hydrogen bonds (Figure 2, figure 3).

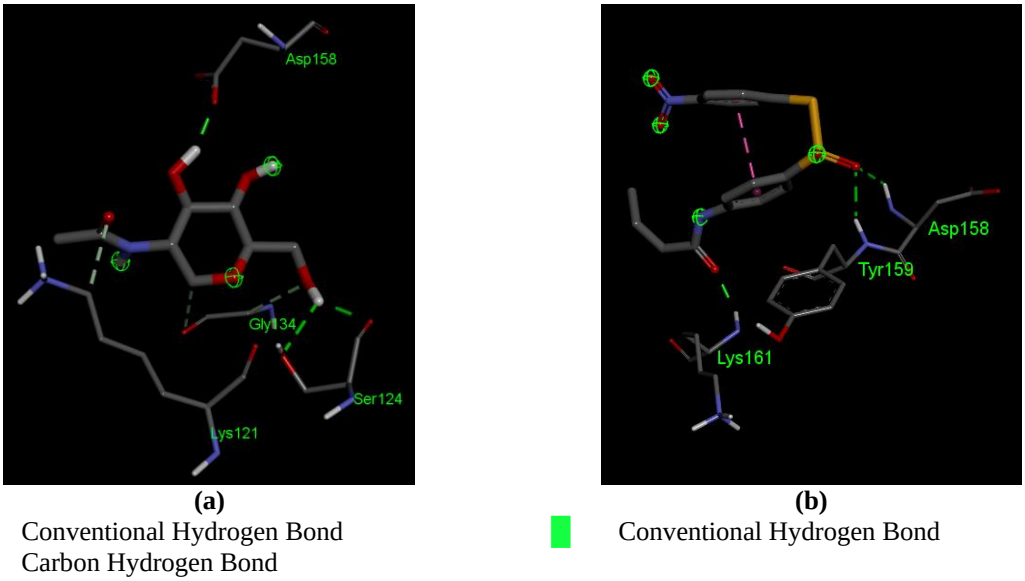

Figure 3. (a) 3D Interactions of the native ligand with target protein 3AL4; (**b**) 3D interactions of **2g** with target protein 3AL4.

The results of screening the biological activity of **1a-1b** and **2a-2g** using molecular docking indicate the high feasibility of searching for new antivirus drugs against COVID-19 targets among the investigated (Table 4). The most promising in this plan of research may be the hit compound "**1a**" - S-Methyl 4-[(trifluoroacetyl)amino]benzenesulfonothioate as well as "**2g**". The affinity value was calculated at a level of -6.3 kcal/mol for both compounds, which was higher than for native ligands: -5.9 kcal/mol (Figure 4, figure 5).

Table 4. The results of the Gscore summary function of the conducted docking studies of given compounds against COVID-19 target 6LU7.

Compound	ligand	1a	1b	2a	2b	2c	2d	2e	2f	2g
Affinity (kcal/mol)	-5.9	-6.3	-6.2	-5.3	-5.7	-5.4	-5.7	-5.6	-6.0	-6.3

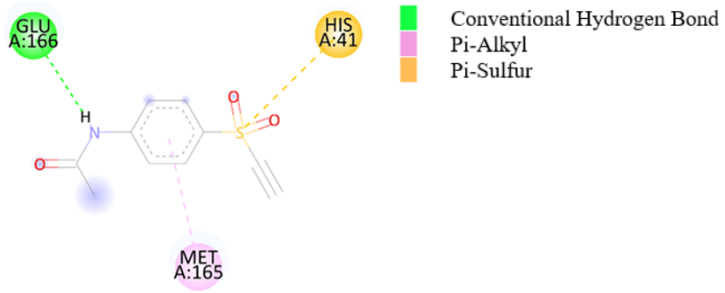

Figure 4. 2D interactions of the native ligand with target protein 6LU7.

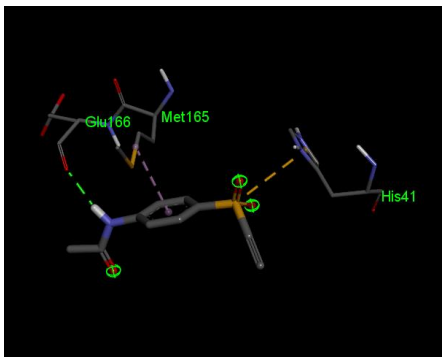

Figure 5. 3D interactions of native ligand with target protein 6LU7.

The nitrophenyl fragment of **2g** is held in the active site by the conventional hydrogen bonds, Pi-Sigma bonds with THR A:25. Nitrophenyl fragment is also held in the active site with Pi-Sulfur bonds with MET A:49. The sulfo group has established a bond with SER A:144, CYS A:145 and with HIS A:41 via conventional hydrogen bonds. CYS A:145 also holds a benzene fragment via an Alkyl bond. 3-chloropropanamide fragment of benzenesulfonothioate is held in an active site of a 6LU7 protein via an unfavorable donor-donor bond with GLU A:166. The Propil fragment is held with a Pi-Alkyl bond with MET A:165 (Figure 6, figure 7).

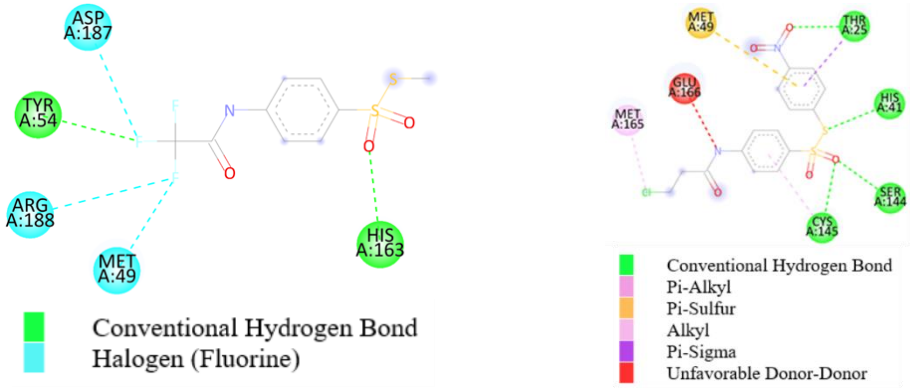

(a) **(b)**

Figure 6 (a) 2D Interactions of **1a** with target protein 6LU7; **(b)** 2D Interactions of **2g** with target protein 6LU7.

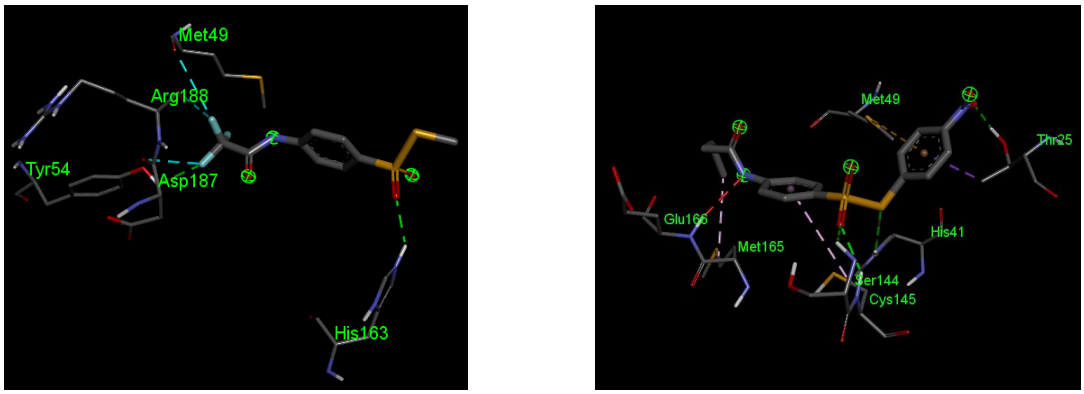

(a) **(b)**

Conventional Hydrogen Bond
Halogen (Fluorine)

Conventional Hydrogen Bond
Pi-Alkyl
Pi-Sulfur
Alkyl
Pi-Sigma
Unfavorable Donor-Donor

Figure 7 (a) 3D Interactions of **1a** with target protein 6LU7; **(b)** 3D Interactions of **2g** with target protein 6LU7.

The sulfo group of **1a** is held in the active site by the conventional hydrogen bonds with HIS A:163. The Fluorine group established a bond with TYR A:54 via conventional hydrogen bonds. It also has Fluorine bonds with ASP A:187, ARG A:188, and MET A:49 (Figure 6).

In Figure 5, we established that the sulfo group is held in the active site via Pi-Sulfur bond with HIS A:41. The 4-aminobenzene-1-thiol fragment is held by Pi-Alkyl bonds with MET A:165. Also, the native ligand is held by a conventional hydrogen bond with GLU A:166.

4. Conclusions

An in silico screening of compounds included in the combinatorial library of those ethers was carried out using the SuperPred web server and AutoDock Vina.

In the process of conducting in silico screening, a lead compound was identified for conducting experimental research in the search for an effective medicinal substance for the treatment of COVID-19 as well as for swine influenza (H1N1). The most promising is "**1a**" - S-Methyl 4-[(trifluoroacetyl)amino] benzenesulfonothioate and "**2g**" - S-(4-Nitrophenyl) 4-[(3-chloropropanoyl)amino] benzenesulfonothioate which proved to be the best in docking studies and showed a high level of affinity with the 6LU7 protein and with 3AL4 protein.

For these compounds, it is advisable to carry out experimental studies of their antiviral activity against COVID-19 and swine influenza (H1N1) because, in addition to the fact that they gave a good forecast of the presence of such activities in them, they also meet all the criteria of drug similarity according to Lipinski's rules.

It is important to mention that, in the screening phase, other compounds with promising anticancer properties were discovered. The compounds, specifically **1b** - S-Ethyl 4-[(trifluoroacetyl) amino] benzenesulfonothioate and **2a** - S-Methyl 4-[(3-chloropropanoyl) amino] benzenesulfonothioate, demonstrated significant activity in treating breast cancer targets, with a probability of 89.64% and 81.28% respectively.

Funding

This research received no external funding.

Acknowledgments

In this section, you can acknowledge any support given that is not covered by the author's contribution or funding sections. This may include administrative and technical support or donations in kind (e.g., materials used for experiments).

Conflicts of Interest

The authors declare no conflict of interest

References

1. Singh, A.K.; Singh, R.; Joshi, S.R.; Misra, A. Mucormycosis in COVID-19: A systematic review of cases reported worldwide and in India. *Diabetes Metab. Syndr.: Clin. Res. Rev.* **2021**, *15*, 102146, https://doi.org/10.1016/j.dsx.2021.05.019.
2. Zheng, Y.; Qing, F.-L.; Huang, Y.; Xu, X.-H. Tunable and Practical Synthesis of Thiosulfonates and Disulfides from Sulfonyl Chlorides in the Presence of Tetrabutylammonium Iodide. *Adv. Synth. Catal.* **2016**, *358*, 3477-3481, https://doi.org/10.1002/adsc.201600633.

3. Vasylyuk, S.; Komarovska-Porokhnyavets, O.; Novikov, V.; Lubenets, V. Modification of alkyl esters of 4-aminobenzenethiosulfonic acid by S-triazine fragment and investigation of their growth-regulative activity. *Chem. Chem. Technol.* **2018**, *12*, 24-28, https://doi.org/10.23939/chcht12.01.024.
4. Zaczynska, E.; Czarny, A.; Karpenko, O.; Vasylyuk, S.; Monka, N.; Stadnytska, N.; Fizer, L.; Komarovska-Porokhnyavets, O.; Jaranowski, M.; Lubenets, V. Obtaining and determining antiviral and antibacterial activity of S-esters of 4-R-aminobenzenethiosulfonic acid. *Chem. Chem. Technol.* **2023**, *17*, 315–324, https://doi.org/10.23939/chcht17.02.315.
5. Halenova, T.I.; Nikolaeva, I.V.; Nakonechna, A.V.; Bolibrukh, K.B.; Monka, N.Y.; Lubenets, V.I.; Savchuk, O.M.; Novikov, V.P.; Ostapchenko, L.I. The search of compounds with antiaggregation activity among S-esters of thiosulfonic acids. *Ukr. Biochem. J.* **2015**, *87*, 83-92, https://doi.org/10.15407/ubj87.05.083.
6. Liubas, N.; Iskra, R.; Kotyk, B.; Monka, N.; Lubenets, V. Prooxidant-antioxidant profile in tissues of rats under the action of thiosulfonate esters. *Ukr. Biochem. J.* **2022**, *94*, 18-29, https://doi.org/10.15407/ubj94.06.018.
7. Dmitryjuk, M.; Szczotko, M.; Kubiak, K.; Trojanowicz, R.; Parashchyn, Z.; Khomitska, H.; Lubenets, V. S-Methyl-(2-Methoxycarbonylamino-Benzimidazole-5) Thiosulfonate as a Potential Antiparasitic Agent—Its Action on the Development of *Ascaris suum* Eggs In Vitro. *Pharmaceuticals* **2020**, *13*, 332, https://doi.org/10.3390/ph13110332.
8. Khodyuk, R.G.D.; Bai, R.; Hamel, E.; Lourenço, E.M.G.; Barbosa, E.G.; Beatriz, A.; dos Santos, E.d.A.; de Lima, D.P. Diaryl disulfides and thiosulfonates as combretastatin A-4 analogues: Synthesis, cytotoxicity and antitubulin activity. *Bioinorg. Chem.* **2020**, *101*, 104017, https://doi.org/10.1016/j.bioorg.2020.104017.
9. Suprovych, T.; Stroianovska, L.; Vishchur, O.; Havryliak, V.; Vasylyuk, S.; Masyuk, M.; Solovodzinska, I.; Lubenets, V. Influence of liposomal thiosulfonate drug on the blood parameters of cows suffering catarrhal mastitis. *Regul. Mech. Biosyst.* **2023**, *14*, 195–202, https://doi.org/10.15421/022329.
10. Lubenets, V.; Vasylyuk, S.; Monka, N.; Bolibrukh, K.; Komarovska-Porokhnyavets, O.; Baranovych, D.; Musyanovych, R.; Zaczynska, E.; Czarny, A.; Nawrot, U.; Novikov, V. Synthesis and antimicrobial properties of 4-acylaminobenzenethiosulfoacid S-esters. *Saudi Pharm. J.* **2017**, *25*, 266-274, https://doi.org/10.1016/j.jsps.2016.06.007.
11. Vira, L.; Nataliya, S.; Diana, B.; Sofiya, V.; Olena, K.; Viktoriya, H.; Volodymyr, N. Thiosulfonates: The Prospective Substances against Fungal Infections. In Fungal Infection, Érico Silva de, L., Juliana Simoni Moraes, T., Eds.; IntechOpen: Rijeka, **2019**; p. Ch. 6.https://doi.org/10.5772/intechopen.84436.
12. Super-PRED. Retrieved from: https://prediction.charite.de/subpages/target_prediction.php. (accessed on 6 11 **2023**).
13. Gallo, K.; Goede, A.; Preissner, R.; Gohlke, B.-O. SuperPred 3.0: drug classification and target prediction—a machine learning approach. *Nucleic Acids Res.* **2022**, *50*, W726-W731, https://doi.org/10.1093/nar/gkac297.
14. Vasylyuk, S.; Shved, O.; Hubrii, Z.; Vichko, O.; Shved, O. Biosafety and biosafety of health and the environment on the basis of information technologies. In CEUR Workshop Proceedings, **2022**; Volume 3309, pp. 109-116.
15. Molinspiration Cheminformatics. Retrieved from: https://www.molinspiration.com. (accessed on 6 11 **2023**).
16. Bai, S.B.; Geethavani, M.; Ramakrishna, C. Synthesis Characterization and Molinspiration Analysis, Anti-bacterial activity of Novel 2,4,6-tri Substituted Pyrimidines. *J. Young Pharm.* **2022**, *14*, 174, https://doi.org/10.5530/jyp.2022.14.33.
17. Pollastri, M.P. Overview on the Rule of Five. *Curr. Protoc. Pharmacol.* **2010**, *49*, 9-12, https://doi.org/10.1002/0471141755.ph0912s49.
18. Dassault Systems. *BIOVIA Discovery Studio.* Available online: https://discover.3ds.com/discovery-studio-visualizer-download. (accessed on 17 10 **2023**).
19. Script Research. Available online: https://autodock.scripps.edu. (accessed on 17 10 **2023**).
20. Ubani, A.; Agwom, F.; Morenikeji, O.R.; Shehu, N.Y.; Umera, E.A.; Umar, U.; Omale, S.; Aguiyi, J.C.; Nnadi, N.E.; Luka, P.D. Molecular docking analysis of selected phytochemicals on two SARS-CoV-2 targets. *F1000Research* **2020**, *9*, 1157, https://doi.org/10.12688/f1000research.25076.1.
21. Thapa, S.; Nargund, S.L.; Biradar, M.S. Molecular Design and In-Silico Analysis of Trisubstituted Benzimidazole Derivatives as Ftsz Inhibitor. *J. Chem.* **2023**, *2023*, 9307613, https://doi.org/10.1155/2023/9307613.

22. Veber, D.F.; Johnson, S.R.; Cheng, H.-Y.; Smith, B.R.; Ward, K.W.; Kopple, K.D. Molecular Properties That Influence the Oral Bioavailability of Drug Candidates. *J. Med. Chem.* **2002**, *45*, 2615-2623, https://doi.org/10.1021/jm020017n.
23. Zhou, Y.; Zhang, Y.; Lian, X.; Li, F.; Wang, C.; Zhu, F.; Qiu, Y.; Chen, Y. Therapeutic target database update 2022: facilitating drug discovery with enriched comparative data of targeted agents. *Nucleic Acids Res.* **2022**, *50*, D1398-D1407, https://doi.org/10.1093/nar/gkab953.
24. Luo, M. Influenza Virus Entry. In *Viral Molecular Machines*, Rossmann, M.G., Rao, V.B., Eds.; Springer US: Boston, MA, **2012**; Volume 726, pp. 201-221, https://doi.org/10.1007/978-1-4614-0980-9_9.
25. Jin, Z.; Du, X.; Xu, Y.; Deng, Y.; Liu, M.; Zhao, Y.; Zhang, B.; Li, X.; Zhang, L.; Peng, C.; Duan, Y.; Yu, J.; Wang, L.; Yang, K.; Liu, F.; Jiang, R.; Yang, X.; You, T.; Liu, X.; Yang, X.; Bai, F.; Liu, H.; Liu, X.; Guddat, L.W.; Xu, W.; Xiao, G.; Qin, C.; Shi, Z.; Jiang, H.; Rao, Z.; Yang, H. Structure of M^{pro} from SARS-CoV-2 and discovery of its inhibitors. *Nature* **2020**, *582*, 289-293, https://doi.org/10.1038/s41586-020-2223-y.
26. Liu, X.; Zhang, B.; Jin, Z.; Yang, H.; Rao, Z. The crystal structure of COVID-19 main protease in complex with an inhibitor N3. *Protein DataBank* **2020**, *10*, https://doi.org/10.2210/pdb6lu7/pdb.
27. Zhang, W.; Qi, J.; Shi, Y.; Li, Q.; Gao, F.; Sun, Y.; Lu, X.; Lu, Q.; Vavricka, C.J.; Liu, D. Crystal structure of the swine-origin A (H1N1)-2009 influenza A virus hemagglutinin (HA) reveals similar antigenicity to that of the 1918 pandemic virus. *Protein Cell* **2010**, *1*, 459-467, https://doi.org/10.2210/pdb3al4/pdb.
28. Xiao, W.; Wang, D.; Shen, Z.; Li, S.; Li, H. Multi-Body Interactions in Molecular Docking Program Devised with Key Water Molecules in Protein Binding Sites. *Molecules* **2018**, *23*, 2321, https://doi.org/10.3390/molecules23092321.
29. Azad, I.; Khan, T.; Maurya, A.K.; Irfan Azad, M.; Mishra, N.; Alanazi, A.M. Identification of Severe Acute Respiratory Syndrome Coronavirus-2 inhibitors through in silico structure-based virtual screening and molecular interaction studies. *J. Mol. Recognit.* **2021**, *34*, e2918, https://doi.org/10.1002/jmr.2918.
30. Naiqing, X.; Tang, X.; Wang, X.; Cai, M.; Liu, X.; Lu, X.; Hu, S.; Gu, M.; Hu, J.; Gao, R.; Liu, K.; Chen, Y.; Liu, X.; Wang, X. Hemagglutinin affects replication, stability and airborne transmission of the H9N2 subtype avian influenza virus. *Virology* **2024**, *589*, 109926, https://doi.org/10.1016/j.virol.2023.109926.